Extension of the hard-sphere model for particle-flow simulations

Pawel Kosinski
University of Bergen, Department of Physics and Technology Bergen, Norway

Boris V. Balakin and Anna Kosinska
Western Norway University of Applied Sciences, Department of Mechanical and Marine Engineering, Bergen, Norway

(Received 22 May 2020; accepted 30 July 2020; published 25 August 2020)

Discrete element methods require appropriate models for particle-particle collisions. Usually, researchers use soft-sphere types of models where the collision dynamics is solved numerically. This makes the simulation computationally expensive. In this paper, however, we show a hard-sphere model that uses ready analytic formulas that relate the pre- and postcollisional velocities of the particles in contact. This hard-sphere model is an extension of an existing model that uses three input parameters. For this, we applied the linear-spring soft-sphere model, where analytic relations can be found. These relations were implemented into the standard hard-sphere model. As a result, we obtain a robust hard-sphere model that is more accurate than the standard one and is still computationally cheap.

DOI: 10.1103/PhysRevE.102.022909

I. INTRODUCTION

Collisions between solid particles are important in, for instance, multiphase flows especially if particle concentrations are high. When modeling such systems, different mathematical models can be used, and perhaps the most common technique is the soft-sphere approach. This approach is especially popular when using discrete element methods.

The soft-sphere model is based on the description of the whole collision dynamics by considering forces acting between particles in contact. We can take into account elastic, inelastic, plastic, and adhesive interactions, as well as more complex phenomena such as liquid bridging. This is the main advantage of this technique. Nevertheless, its main drawback is a high-computational cost, because it requires solving the main equations numerically. The development of the soft-sphere approach and discussion can be found in many references such as Refs. [1–10], while some selected examples of its use are [11–13] among many others.

Another approach, less common, is the hard-sphere approach that is a result of solving impact equations: this makes the computation to be significantly faster because the obtained relations are analytic. Nevertheless, the existing hard-sphere models do not consider many physical phenomena and therefore may be less applicable.

There are different versions of the hard-sphere model that can be found in the literature. The first one is the case where the colliding particles are assumed to be frictionless, see, e.g., Refs. [14–16]. In this case, one input parameter is needed, namely the coefficient of restitution that is usually defined as the ratio of the relative velocity of the colliding particles along the normal to the plane of impact at the end of the collision to the same velocity measured before the collision.

The second case is a model involving two input coefficients: a normal and a tangential coefficient of restitution. This type of model is often used in computational fluid dynamics software. Selected examples are Refs. [17–21].

The next model uses two input parameters: the normal coefficient of restitution and the coefficient of friction. Therefore, in the following, we refer to it as a "two-parameter hard-sphere model". The details of the model can be found in many references starting with very early works, e.g., Ref. [22]. The model is based on detailed investigation of collision dynamics between two bodies of arbitrary shape (i.e., not necessarily spherical), see, e.g., Refs. [23–29]. It has also been used for multiphase flow applications and is in this context mentioned in, for instance, Refs. [30–33].

Finally, there exists a hard-sphere model that uses three input parameters, called in this paper as a "three-parameter hard-sphere model". In addition to the two parameters mentioned in the previous paragraph, it uses a third one that can be called the limiting tangential coefficient of restitution for nonsliding collisions. This model was initially described in detail in Ref. [34] and later was widely used by many researchers, e.g., Refs. [35–37]. This model is a basis of the present paper so we recapitulate it in subsequent sections.

In the end, we mention shortly attempts to include cohesive forces into the hard-sphere model. An example is the paper by Weber *et al.* [16,38], who introduced a particle interaction potential to the aforementioned model for frictionless collisions. The issue of cohesion was studied in our own research [39], where the two-parameter hard-sphere model for particle-wall collisions was extended. In this model, a cohesive impulse was introduced that accounts for the attractive interaction. A similar approach was also later used in Refs. [32,40] for particle-particle collisions.

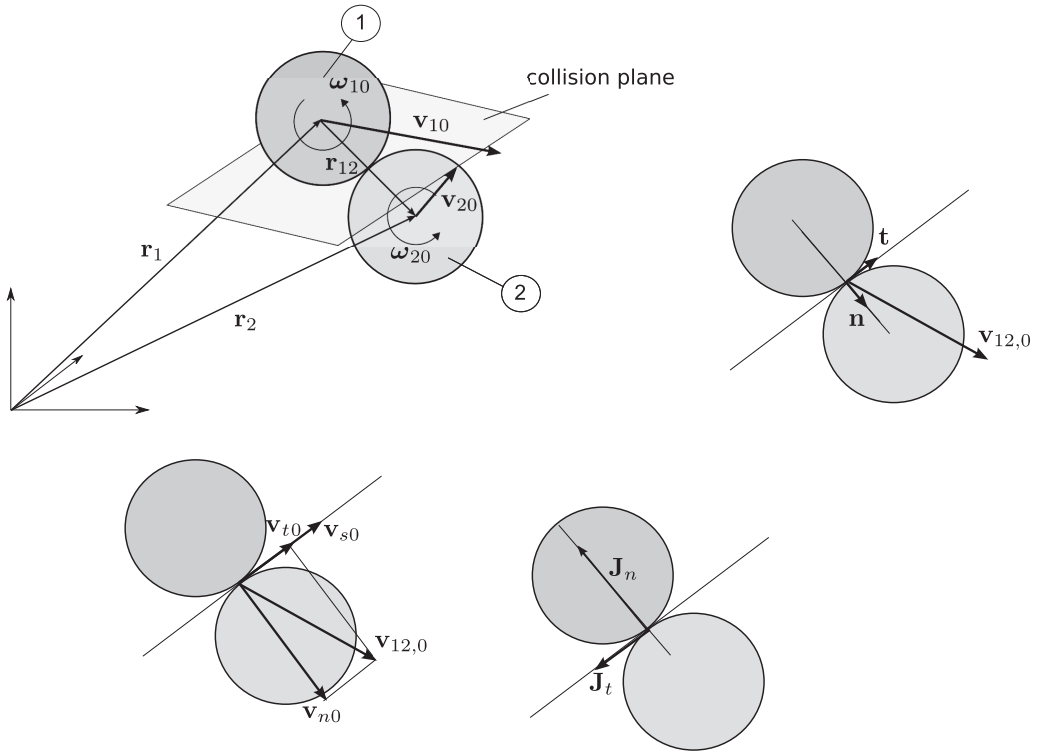

FIG. 1. Collision dynamics.

II. OBJECTIVE OF THE PAPER

The main goal of this paper is an extension of the most complex of the previously mentioned hard-sphere models, namely the three-parameter hard-sphere model. The model uses the following input parameters: (i) the normal coefficient of restitution e, (ii) the coefficient of friction for sliding collisions f, and (iii) the limiting tangential coefficient of restitution β_o. In many practical applications, as well as in research papers, these three parameters have been assumed to be constant for specific particle properties. As a matter of fact, it is usually not a case especially for the first and the third parameter.

Nevertheless, there are different analytic relations for the normal coefficient of restitution, see, e.g., Refs. [41–45], which take into account the precollisional velocity so that they can be easily applied in the hard-sphere model.

For the third parameter (β_o) however, such relations rather do not exist and therefore users of the model usually assume that this parameter is constant and found empirically. This approach is essentially not correct, as shown later in the paper, and our objective is to avoid this drawback.

Our strategy can be summarized as follows: we combine the three-parameter hard-sphere model with a soft-sphere approach based on the linear-spring approach. By using the soft-sphere analysis of the collision process, we find the relative sliding velocity at the end of the collision, which can replace the parameter β_o. For elastic collisions (i.e., when the coefficient of restitution is equal to 1.0) the methodology developed in Ref. [46] was used in this paper.

As a result, we find *analytic* relations that can readily be used in the hard-sphere model. The extended hard-sphere model is validated against benchmarks, that is, soft-sphere simulations and some selected experiments available in the literature. This model is valuable for both researchers working on fundamental aspects of particle-particle interactions and for engineers looking for efficient and computationally cheap models.

Next, we use a more complex soft-sphere model that does not lead to analytic relations, especially for inelastic collisions. Still, by exploiting the technique of dimensional analysis, we develop semiempirical relations that can be later used.

III. SUMMARY OF THE THREE-PARAMETER HARD-SPHERE MODEL

This model was initially described in detail in Ref. [34]. Nevertheless, in the present section, it is briefly summarized because it forms a base for further development. The reader may find other details in the cited reference.

Figure 1 shows a collision of two spherical particles that are denoted with numbers "1" and "2". The locations of the particle centres are denoted with vectors $\mathbf{r}_1$ and $\mathbf{r}_2$. Masses, diameters and moments of inertia are m_1, m_2, d_1, d_2, I_1, and I_2 while linear and angular velocities before impact are $\mathbf{v}_{10}$, $\mathbf{v}_{20}$, $\boldsymbol{\omega}_{10}$, and $\boldsymbol{\omega}_{20}$.

A unit vector, $\mathbf{n}$, normal to the plane of collision and directed towards particle "2" is defined. A unit vector, $\mathbf{t}$, tangential to the plane of collision and in the direction of the projection on the plane of the precollisional relative velocity $\mathbf{v}_{12,0} = \mathbf{v}_{10} - \mathbf{v}_{20}$ is also specified. These unit vectors can be used for finding the vectors of the precollisional relative velocity normal and tangential to the plane of collision,

$\mathbf{v}_{n0}$ and $\mathbf{v}_{t0}$. The latter can then be used for calculating the relative surface velocity in the tangential direction just before the collision: $\mathbf{v}_{s0} = \mathbf{v}_{t0} - d_1/2(\mathbf{n} \times \boldsymbol{\omega}_{10}) - d_2/2(\mathbf{n} \times \boldsymbol{\omega}_{20})$ with magnitude $v_{s0} = \mathbf{v}_{s0} \cdot \mathbf{t}$. The vertical and tangential components of $\mathbf{v}_{12,0}$ are $v_{n0} = \mathbf{v}_{12,0} \cdot \mathbf{n}$ and $v_{t0} = \mathbf{v}_{12,0} \cdot \mathbf{t}$; with the definitions given, these components are always positive.

The postcollisional velocities of the particles can be found from the linear and angular impulse equations for the collision:

$$\mathbf{v}_1 = \mathbf{v}_{10} + (J_n\mathbf{n} + J_t\mathbf{t})/m_1, \tag{1a}$$

$$\mathbf{v}_2 = \mathbf{v}_{20} - (J_n\mathbf{n} + J_t\mathbf{t})/m_2, \tag{1b}$$

$$\begin{aligned}\boldsymbol{\omega}_1 &= \boldsymbol{\omega}_{10} + d_1/2 \cdot \mathbf{n} \times (J_n\mathbf{n} + J_t\mathbf{t})/I_1 \\ &= \boldsymbol{\omega}_{10} + d_1 J_t/(2I_1)(\mathbf{n} \times \mathbf{t}),\end{aligned} \tag{1c}$$

$$\begin{aligned}\boldsymbol{\omega}_2 &= \boldsymbol{\omega}_{20} + d_2/2 \cdot \mathbf{n} \times (J_n\mathbf{n} + J_t\mathbf{t})/I_2 \\ &= \boldsymbol{\omega}_{20} + d_2 J_t/(2I_2)(\mathbf{n} \times \mathbf{t}),\end{aligned} \tag{1d}$$

where J_n and J_t are components of the impulse $\mathbf{J}$ that acts on the particle "1". Thus, if J_n and J_t were known, the postcollisional velocities could readily be found. Therefore, the main issue is to find these two components.

In the hard-sphere model the normal component of impulse, J_n, is found by introducing the normal coefficient of restitution, the value of which is given as an input parameter:

$$e = -\frac{\mathbf{n} \cdot \mathbf{v}_{12}}{\mathbf{n} \cdot \mathbf{v}_{12,0}} = -\frac{v_n}{v_{n0}}, \tag{2}$$

and thus

$$J_n = \mathbf{n} \cdot \mathbf{J} = -m_*(1 + e)v_{n0} < 0, \tag{3}$$

where m_* is the effective mass defined as $m_1 m_2/(m_1 + m_2)$. This shows that J_n can be easily computed.

The quantification of the tangential component of the impulse, J_t depends on the type of collision and the model used as discussed in the next paragraphs. The first possibility is that particles slide during the entire collision so that J_t can be related to J_n by Coulomb's law of friction:

$$J_t = fJ_n < 0, \tag{4}$$

where f is the coefficient of friction, which is given as an input to the model. Thus the unknown parameters are determined and the postcollisional linear and angular velocities can be computed from Eqs. (1).

As mentioned, this applies only to the case where the particles slide over each other during the entire contact. In the following, we refer to this mode as *case 1*.

If the assumption represented by the inequality in Eq. (4) is, however, not valid, we refer to this mode as *case 2*. In order to solve this case, we write the relation for postcollisional relative surface velocity in the tangential direction:

$$\mathbf{v}_s = \mathbf{t}\left(v_{s0} + \frac{7J_t}{2m_*}\right), \tag{5}$$

which can be found using the relations discussed previously.

Next, a parameter referred to as "the coefficient of tangential restitution" is defined as follows:

$$\beta = -\frac{v_s}{v_{s0}}. \tag{6}$$

β for case 1 can be found using Eq. (5), the relation $\mathbf{v}_s = v_s\mathbf{t}$ and Eqs. (3) and (4):

$$\beta = -1 + \frac{7}{2}f(1 + e)\frac{v_{n0}}{v_{s0}}. \tag{7}$$

In the studied three-parameter model, the surface velocity decelerates from v_{s0} until it reaches v_s at the end of collision. It means that if sliding takes place during the whole contact, β remains low, see Eq. (7). In the model, β is permitted to take on positive values up to a limit, β_0 (where $0.0 < \beta_0 < 1.0$), which is given as an input parameter [34]. If β remains less than β_0 during the collision then sliding takes place during the whole collision process and the postcollisional velocities can be found from Eqs. (1) using Eqs. (3) and (4), as already mentioned.

For the case where the calculated β exceeds β_0, β is assumed to take on the value of β_0 [34]. Here, we use Eq. (6) and by combining with Eq. (5), a tangential impulse that corresponds to this limit can be found:

$$J_t = -\tfrac{2}{7}m_* v_{s0}(\beta_0 + 1). \tag{8}$$

Substituting J_t in Eqs. (1) gives postcollisional velocities that are valid for the cases where the calculated β exceeds β_0. Similarly to case 1, J_n is computed from Eq. (3).

As discussed before the main issue is the value of the parameter β_0 that is usually assumed to be an empirical constant. It has been shown in this section that the main issue is v_s for the case where the surfaces stop sliding somewhere during contact. In the previously mentioned two-parameter hard-sphere model v_s is assumed to be zero in this case, while in the three-parameter hard-sphere model v_s becomes $-v_{s0}\beta_o$. Nevertheless, a question that can be asked is whether it is not possible to find v_s using another strategy. In such a case, β can be directly calculated from Eq. (6), and then J_t can be found from Eq. (8) by replacing β_0 with β.

This is an issue studied in this paper and a potential solution to the problem is shown in the following sections.

IV. SUMMARY OF THE ANALYTIC SOLUTION OF THE LINEAR-SPRING SOFT-SPHERE MODEL FOR ELASTIC COLLISIONS

The first model studied in the present paper is the linear-spring model as described by Cundall and Strack [1] and later it was intensively used for various practical applications. Recently it has been also revisited in, e.g., Refs. [5,6,9,10].

In the present paper, we do not repeat the details of the model, since they are available in the literature, especially in Cundall and Strack [1]. We only show the main relations.

At first, we refer again to Fig. 1 that shows a collision of two particles. This time we investigate the deformation of the particle surfaces along the normal to the plane of impact. This deformation is denoted as δ_n. Similarly one may define a deformation along the tangential, δ_s. The general equation of motion for, e.g., along the normal to the plane of impact is: $m_*\ddot{\delta}_n = -k_n\delta_n$, with k_n being a spring constant.

The displacement increments during contact are: $\Delta\delta_n = v_n\Delta t$ and $\Delta\delta_s = v_s\Delta t$, respectively, where v_n and v_s are current (i.e., functions of time during the course of collision) values of the normal and the tangential components of the

relative velocity, and Δt is time step. It must be noted that in the previous section (i.e., for the hard-sphere model), this information was not available, that is, the hard-sphere model was based on using only the initial and the final values of velocity.

The displacement increments can be used in each time step for calculating the increments of the normal and tangential components of force, where in the linear model by Cundall and Strack they become $\Delta F_n = k_n \Delta\delta_n$ and $\Delta F_t = k_t \Delta\delta_s$ with the constant parameters k_n and k_t being material dependent. This makes it possible to find values of the force components for a new time step: $(F_n)^{m+1} = (F_n)^m + \Delta F_n$ and $(F_t)^{m+1} = (F_t)^m + \Delta F_t$.

Having found forces for the next time step, the friction-law is invoked: if the calculated force F_t is greater than fF_n, where f is the coefficient of friction (compare with the previous section), than F_t is set to fF_n. The new values of the force components are used to find the velocity components and locations of the particles in the new time step.

The course of collision can be predicted, see, e.g., Refs. [5,47], by using a parameter ψ_0 that is

$$\psi_0 = \frac{\kappa}{f}\frac{v_{s0}}{v_{n0}}, \tag{9}$$

where v_{s0}/v_{n0} is so-called impact angle ($\equiv \tan\alpha$) and $\kappa = k_t/k_n$.

When the angle of impact, defined as the angle between the normal to the plane of impact and the relative velocity vector, is high the collision occurs entirely in the so-called gross sliding range. This situation occurs when $\psi_0 > 7\kappa - 1$ and in the following we refer to it as case (a).

As the impact angle becomes lower the course of collision also changes. In the beginning, the gross sliding is observed and after that, it stops so that the surfaces deform when being in contact. At the end of the collision, however, the gross sliding occurs again, since the normal force acting between the particles becomes smaller. This situation occurs when $1 < \psi_0 \leqslant 7\kappa - 1$ and in the following we refer to it as case (b).

For very small impact angles there is no initial gross sliding since the normal force is high. Nevertheless, at the end of collision, gross sliding applies again. This case occurs for $\psi_0 \leqslant 1$ and also is embedded into case 2 for the hard-sphere model. This situation is called case (c) later in the paper.

It should be noted that case (a) corresponds entirely to case 1, defined in the section on the hard-sphere model. Similarly case (b) and (c) can be treated as equivalent to case 2, even though the standard hard-sphere model does not describe the details of the process.

The whole model can be solved numerically, but it can also be solved analytically as shown in Ref. [46]. This solution is necessary for the present paper and therefore in the following, the most important findings are repeated. Here we select only these of their results that are later used in the paper. All the other details and derivation can be found in Ref. [46].

For case (c) the final sliding velocity of the contact point is calculated in Ref. [46] as

$$v_s = v_{s0}\cos(\omega_s t_2) + \tfrac{7}{2} v_{n0} f[1 + \cos(\omega_n t_2)], \tag{10}$$

where $\omega_s = \sqrt{7/2k_n/m_*}$ and $\omega_n = \sqrt{k_t/m_*}$. Also t_2 is the point in time (measured during particle-particle contact) in which the change of the mode from sticking to gross sliding takes place. This is found from

$$t_2 = \frac{(A'-1) + \sqrt{(A'-1)^2 + 2\omega_s^2 A^2}}{\omega_s^2 A} + \frac{\pi}{\omega_n}, \tag{11}$$

where

$$A = \frac{\psi_0}{\omega_s}\sin\left(\pi\frac{\omega_s}{\omega_n}\right) \tag{12}$$

and

$$A' = \psi_0\cos\left(\pi\frac{\omega_s}{\omega_n}\right). \tag{13}$$

For case (b) the sliding velocity at the end of collision is found from

$$v_s = v_{s0}^*\cos(\omega_s t_2) - \delta_{s0}^*\omega_s\sin(\omega_s t_2) + \tfrac{7}{2} v_{n0} f[1 + \cos(\omega_n t_2)], \tag{14}$$

where

$$\delta_{s0}^* = \frac{f v_{n0}}{\omega_n \kappa}\sin(\omega_n t_1)\cos(\omega_s t_1) - \frac{\sin(\omega_s t_1)}{\omega_s}\left\{v_{s0} - \frac{7}{2} f v_{n0}[1 - \cos(\omega_n t_1)]\right\} \tag{15}$$

and

$$v_{s0}^* = \left\{v_{s0} - \frac{7}{2} f v_{n0}[1 - \cos(\omega_n t_1)]\right\}\cos(\omega_s t_1) + \frac{f v_{n0}}{\omega_n \kappa}\sin(\omega_n t_1)\omega_s\sin(\omega_s t_1). \tag{16}$$

For case (b) time t_1 corresponds to change from gross sliding to sticking and t_2 from sticking to gross sliding later during collision. These points in time can be found from

$$t_1 = \frac{1}{\omega_n}\cos^{-1}\left[\frac{7/2\kappa - \psi_0}{7/2\kappa - 1}\right], \tag{17}$$

while t_2 can be calculated again from Eq. (11), but this time parameters A and A' are

$$A = \frac{\kappa v_{s0}^*}{\omega_s f v_{n0}}\sin\left(\pi\frac{\omega_s}{\omega_n}\right) + \frac{\kappa\delta_{s0}^*}{f v_{n0}}\cos\left(\pi\frac{\omega_s}{\omega_n}\right) \tag{18}$$

and

$$A' = \frac{\kappa v_{s0}^*}{f v_{n0}}\cos\left(\pi\frac{\omega_s}{\omega_n}\right) - \frac{\kappa\delta_{s0}^*\omega_s}{f v_{n0}}\sin\left(\pi\frac{\omega_s}{\omega_n}\right). \tag{19}$$

In this way, it is possible to predict the sliding velocity v_s at the end of collisions. Note that this value is of importance for the three-parameter hard-sphere model. Therefore, we can attempt to combine both approaches and the details are shown in the next section.

V. EXTENSION OF THE HARD-SPHERE MODEL FOR ELASTIC-FRICTIONAL COLLISIONS

The analytic solution shown in the previous section makes it possible to find the sliding velocity at the end of collision for the case where the particles stop sliding during contact,

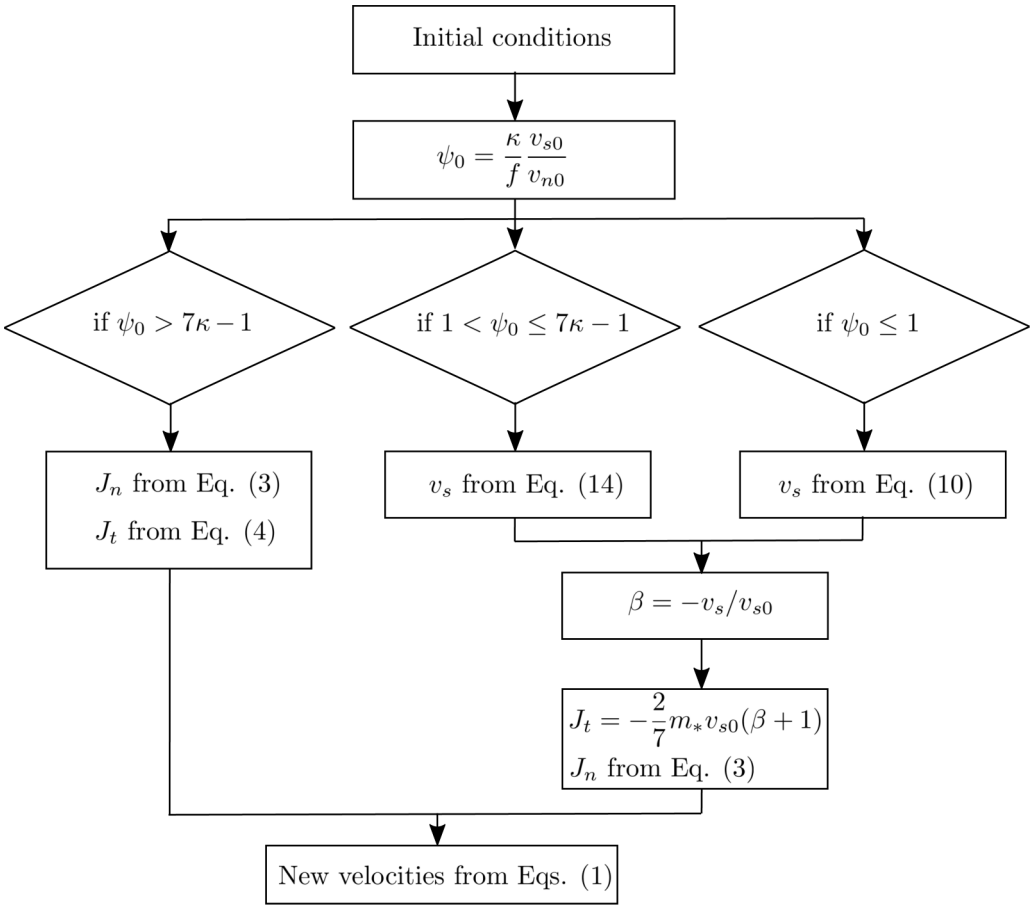

FIG. 2. Collision dynamics.

that is, for case 2 in the hard-sphere model. In other words, it is not necessary to introduce parameter β_o as it is done in the standard hard-sphere model.

Assuming that particle properties, and their precollisional velocities are known, it is possible to build an algorithm for finding the postcollisional velocities using solely analytic relations. We show the algorithm in Fig. 2.

In this way, we obtain a model that is as computationally efficient as the standard hard-sphere model, and at the same time its precision can be compared to the soft-sphere model.

VI. MODEL VALIDATION AND SENSITIVITY ANALYSIS

At first, for model validation we use the same experimental setup as in the paper by Kharaz *et al.* [48], also discussed in Ref. [46]. In these experiments, a spherical particle of size 5 mm were dropped on a solid surface. Various angles of impact were investigated by rotating the surface, where angle 0 degrees corresponded to a vertical collision. The material properties of the particle and the surface resulted in κ being equal to 0.859, the friction coefficient was assumed to be $f = 0.092$ and the coefficient of restitution was 0.98, i.e., almost 1.0, so that the collision can be considered as elastic. The impact speed was 3.9 m/s.

Our model can be used for collisions of particles of different sizes. Here, however, we selected one of the particles to be very large in order to mimic a wall, that is, a few orders of magnitude bigger.

In the following, we compare the hard-sphere model described in the paper with the experimental results from Ref. [48], as well as with the soft-sphere model by Tsuji *et al.* [3]. The soft-sphere model was solved using the numerical scheme shown previously with a time step 10^{-8}s. Since we considered only a single collision, the time step was not optimized even though larger time steps would result in a good performance as well.

We illustrate the course of collision by analyzing the history of the sliding velocity v_s and of the angular velocity of the colliding particle. The results are shown in Fig. 3. We selected four impact angles: 5, 10, 20, and 30 degrees, because these angles comprise different colliding regimes.

The largest angle corresponds to the case where the particle slides all the time during the collision. Close to the end of the collision, we observe that the sliding velocity becomes negative. The reason is that the soft-sphere model considered loading of a "spring" from the start of the process, and unloading at the end.

It must be noted that the aforementioned two-parameter hard-sphere model assumes the final sliding velocity to be zero for the case if the particle slides during the whole course of the collision. This is corrected in the three-parameter model that allows the velocity to become negative by using parameter β_0. On the other hand, it is rather incorrect to use

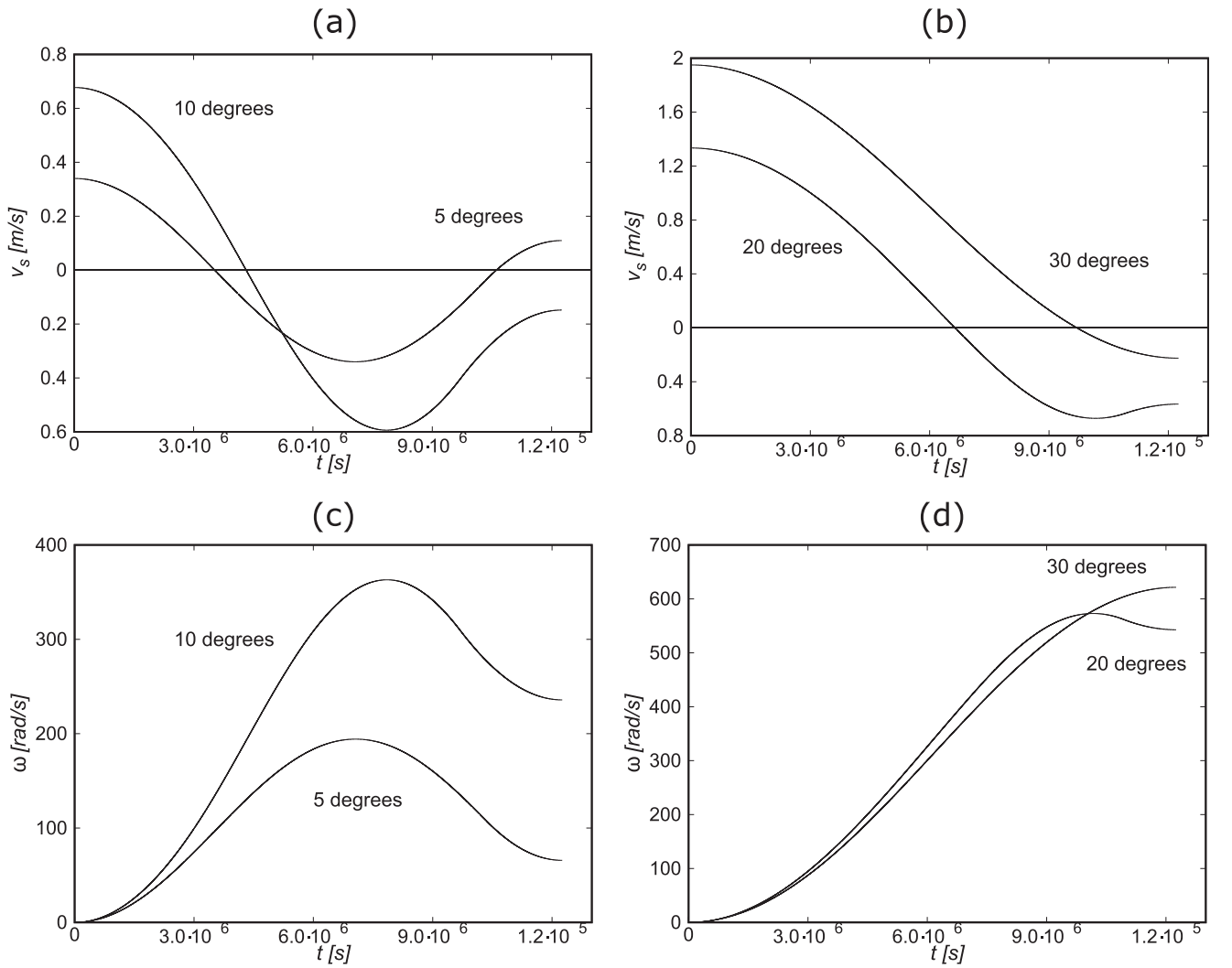

FIG. 3. History of the sliding velocity (a), (b) and the angular velocity (c), (d) of the colliding particle, obtained by the soft-sphere model. The figure compares four cases with the impact angles equal to 5, 10, 20, and 30 degrees.

any constant value for this parameter, as seen from the results. The reason is that the ratio between the final sliding velocity to the initial one depends on the impact angle.

We also note that for the lowest value of the impact angle, i.e., 5 degrees, no sliding occurs. In fact, the sliding velocity has a positive direction at the end of the process. This shows oscillations of the "spring" in the model.

The angular velocity is zero at the beginning of the process and increases to some positive values due to a torque acting on the particle during contact. Close to the end of the contact, it decreases as the tangential force changes its sign. This is especially visible for the lowest impact angles.

Figure 4 shows the final angular velocity of the colliding particle after the collision with the wall. It is clear that for the lowest collision angles (i.e., almost head-on collision), the final angular velocity is the lowest as expected. For larger values of the collision angle, the final angular velocity gradually increases until some maximum value around 30°.

The figures compare five different results. The boxes show the experiments by Kharaz *et al.* At first, we can compare them to the dashed curve, which corresponds to the results obtained

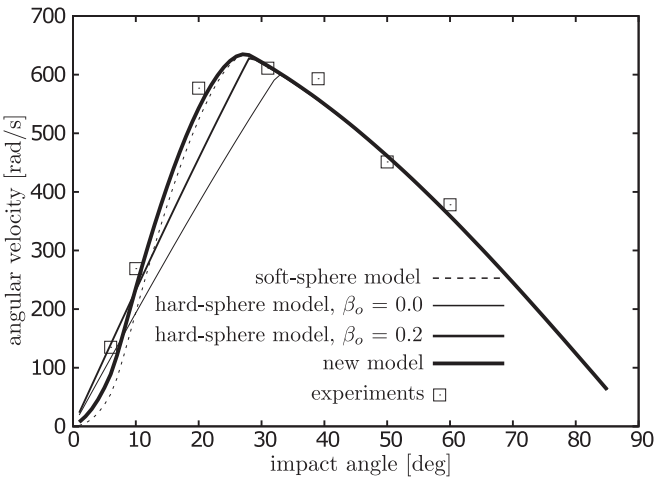

FIG. 4. Postcollisional angular velocity vs impact angle obtained using different models and experiments from Kharaz *et al.* [48]. It is clear that our model, shown in the paper, gives better results if compared with the standard hard-sphere model.

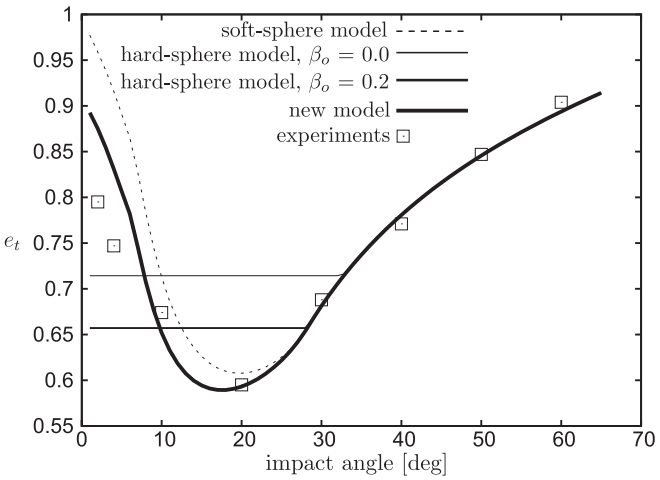

FIG. 5. Tangential coefficient of restitution vs impact angle obtained using different models and experiments from Kharaz *et al.* [48].

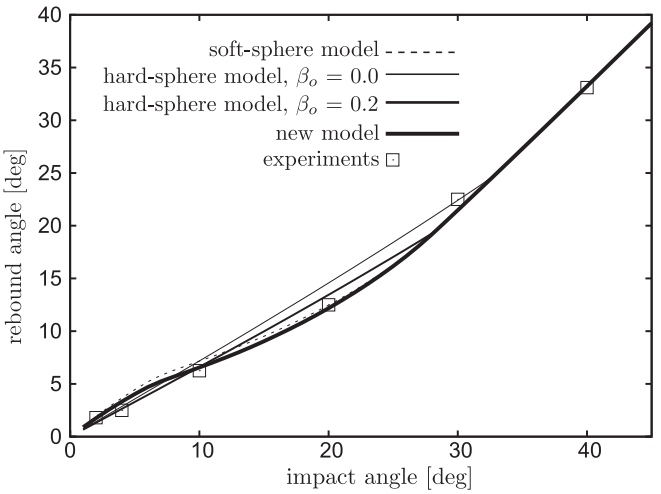

FIG. 6. Particle rebound angle vs impact angle obtained using different models and experiments from Kharaz *et al.* [48].

by the soft-sphere model. This model can be treated as the most accurate, but also the most computationally expensive, as indicated previously in the paper. We see from the figure that the results follow the experiments well.

Next, we analyze the two thin curves that are the standard three-parameter hard-sphere model with two values of parameter β_o: 0.0 and 0.2. It must be noted that the value 0.0 corresponds also to the standard two-parameter hard-sphere model. We see that both cases match the experiments/soft-sphere model for the large impact angles. For these angles, the contact between the colliding surfaces is fully sliding, so that it is not necessary to use parameter β_o at all. For smaller angles, however, there is some discrepancy between the experiments/soft-sphere model, which indicates that β_o should not really be selected as a constant parameter.

Finally, the results obtained by our new hard-sphere model are shown as a thick curve. Obviously, the results follow the benchmark cases, for all the values of the colliding angle.

Analyzing the impact angle 20° as an example, the discrepancy between the modeling results and the experiments is 6% for our model, 10% for the soft-sphere model, 21% for the three-parameter model with $\beta_o = 0.2$, and 34% for the three-parameter model with $\beta_o = 0.0$. This illustrates the robustness of the model.

Similarly, we can investigate also other results and validate the models against the experiments by Kharaz *et al*. Figure 5 shows the measured coefficient of restitution in the tangential direction calculated as $e_t = v_t/v_{t0}$. We remind the reader here that some hard-sphere models use this parameter as a constant input.

According to Fig. 5, the parameter is obviously not constant. Again, the soft-sphere model and the model presented in this paper give the best correspondence to the experimental results. The standard hard-sphere model gives the best accuracy only for the highest angles of impact. For lower angles, the resulting coefficient of restitution in the tangential direction becomes constant and depends on the selection of β_o. This indicates that the standard model should be used with caution if particle-particle interactions are of importance in computer simulations.

Next, Fig. 6 shows the rebound angle after the collision. As expected, lower (higher) impact angles result in higher (lower) rebound angles, because the initial angular velocity was zero. According to the figure, all the models correspond relatively well to the experiments. Nevertheless, the most accurate results were obtained by the soft-sphere model and by our model.

Our model seems to be closer to the experimental results if compared with the soft-sphere model. Nevertheless, this does not need to be the case if slightly different empirical parameters were used in the modeling. Also, the experimental results are associated with some experimental errors, which were not studied.

In the next test, we validate the simulation results against experiments carried out in Ref. [35], where collisions of acetate spheres on an aluminum plate were investigated. The process was simulated in Ref. [49] and we follow their simulation setup. The particle size was 6 mm in diameter, their material had density 1319 kg/m^3. The plate density was 2700 kg/m^3. The friction coefficient was estimated to be 0.208 and the constants k_n and k_t were estimated to be 5.8972×10^5 N/m and 4.7384×10^5 N/m, respectively.

Similarly to Ref. [49] we show the results on graph ψ_2 vs ψ_1, where

$$\psi_1 = \frac{v_{s0}}{v_{n0}} \quad \text{and} \quad \psi_2 = \frac{v_s}{v_{n0}}, \tag{20}$$

where v_s is the relative surface velocity at the end of collision.

Similar to the previous test, we present a series of results of many simulations where the impact angle varied. The results are depicted in Fig. 7 and are compared to the experiments from Ref. [35].

It is interesting to note that the soft-sphere model and our model lead to very close results so that they visually merge in Fig. 7. These results also compare well with the experiments. The three-parameter hard-sphere model, i.e., when $\beta_o = 0.2$, seems to give better results than the two-parameter hard-sphere model (with $\beta_o = 0.0$). It must be, however, noted

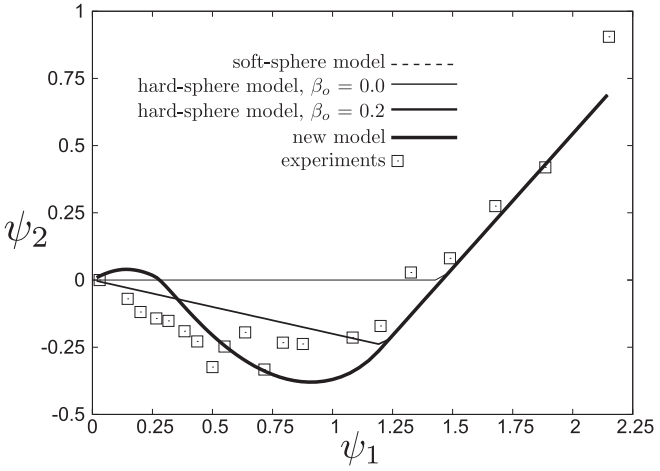

FIG. 7. ψ_2 vs ψ_1 obtained using different models and experiments from Foerster *et al.* [35]. The results from the soft-sphere model and this model are close to each other so that the curves merge.

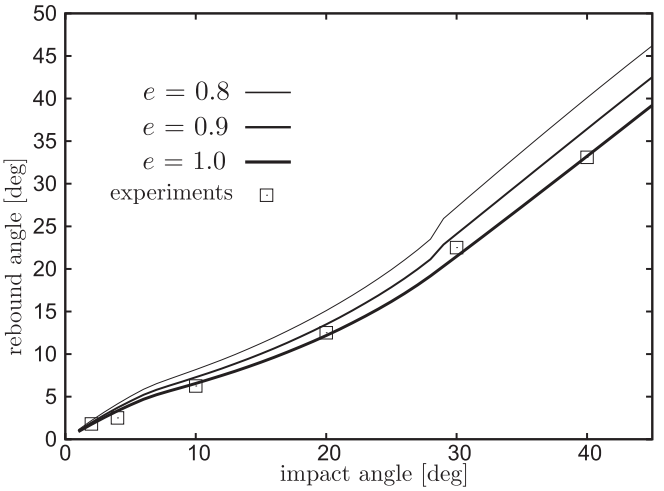

FIG. 8. Particle rebound angle vs impact angle obtained using different values of the normal coefficient of restitution.

that the coefficient β_o is generally unknown so that use of the standard hard-sphere model may lead to some difficulties here.

As previously mentioned, this model is computationally less expensive because it is based on analytical relation and there is no need to solve the collision process numerically, as it is done in the soft-sphere model. In our further tests, we ran our simulation codes for a system in which 6500 collisions occurred. We used one CPU core (Intel E5-2683v4 2.1 GHz). The codes were not optimized.

Our hard-sphere model needed 6 ms to perform the task, while the soft-sphere model needed 4.8 seconds, that is, 800 times longer. It must be noted that the numerical scheme could be improved by using a higher-order scheme and a lower time step. Nevertheless, the difference will still be significant.

VII. POTENTIAL EXTENSION TO INELASTIC-FRICTIONAL COLLISIONS

The model shown in the previous sections describes elastic-frictional collisions, that is, the coefficient of restitution along the normal to the plane, e, of impact is equal to 1.0. For the case when collisions are not elastic, the model cannot be formally used because it uses analytic relations obtained from the linear spring model, where no dissipation is included.

For the soft-sphere approach, inelastic collisions can be modeled by using dissipative terms in the equation of motion. This can be done by mimicking a dashpot in a system with a linear spring. Thus, the equation of motion in the direction normal to the plane of impact becomes $m_*\ddot{\delta}_n = -k_n\delta_n - c_n\dot{\delta}$. It is interesting to note that the damping coefficient can be related to the coefficient of restitution (see, e.g., Ref. [7]):

$$e = \exp\left(-\pi\frac{\beta_n}{\sqrt{1-\beta_n^2}}\right), \tag{21}$$

where $\beta_n = c_n/(2\sqrt{m_* k_n})$, which makes it possible to compare the soft-sphere and the hard-sphere models directly.

Nevertheless, the main difficulty is the lack of analytic solutions for the final sliding velocity v_s for inelastic collisions. As a matter of fact, there have been attempts in literature to solve these types of collisions analytically, where a typical example is Ref. [49], but still, the ready formulas are not available.

Therefore, there are two strategies that can be considered. The first method is based on the assumption that for inelastic collisions where e is relatively close to 1.0, our model can still be used. In other words, the analytic relations for v_s can be applied anyway. The introduced error will probably not influence the results significantly and can be used in engineering applications.

We illustrate this approach in Fig. 8, where we do the same computer simulations as shown in Fig. 6. This time, however, we varied the coefficient e. As we see, this coefficient does not influence the results significantly at least for the studied cases.

This shows that users of our model can consider whether it can be used for their case, taking into account the main advantage, which is the low computational cost.

The second strategy is based on the method already tested by us in our previous works, see, e.g., Refs. [50,51]. Here, we use the dimensional analysis to obtain a semianalytic relation for the final sliding velocity that can be later used in the hard-sphere model. At first, we use again the model with the dashpot as mentioned above, that is, we use the coefficient c_n that accounts for dissipation during particle-particle contact. It means that v_s (that we wish to find) can be considered to depend on

$$v_s = f(v_{n0}, v_{s0}, k_n, k_t, c_n, m_*, f). \tag{22}$$

By using Buckingham Π-theorem [52] the relation can be arranged in a series of dimensionless groups:

$$\frac{v_s}{v_{n0}} = f\left(\psi_0, \kappa, \frac{k_n m_*}{c_n^2}, f\right). \tag{23}$$

Next a functional form of this relation can be found from a set of soft-sphere numerical experiments of a colliding particle-particle pair, for instance, in the following form:

$$\frac{v_s}{v_{n0}} = a_o \psi_0^{a_1} \kappa^{a_2} \left(\frac{k_n m_*}{c_n^2}\right)^{a_3} f^{a_4}, \tag{24}$$

where a_o, a_1, a_2, a_3, a_4 are coefficients. The dimensionless groups should vary in ranges that are relevant for a studied case.

The obtained relation can be implemented into a computer code that is used for simulations of systems with many particles. This makes it possible to run simulations that are not computationally expensive.

VIII. CONCLUDING REMARKS

The focus of this paper was on the formulation of a different hard-sphere model, where as an input we used the linear-spring soft-sphere model. This led to very promising results: a better accuracy than the standard hard-sphere model and a low computational cost.

It must be mentioned that the linear-spring model is relatively simple. In reality, particle-particle interactions are more complex. The relation between the elastic force acting on the particles and their displacement is not linear and should be rather described by, e.g., Hertz theory. There exist soft-sphere models that take into account more physically correct effects, e.g., Refs. [3,4,53,54] to name a few. These models are detailed but do not offer ready analytic solutions that can be easily implemented into the hard-sphere model.

ACKNOWLEDGMENTS

This study was supported by the Norwegian Research Council (Project No. 300286).

[1] P. A. Cundall and O. D. L. Strack, A discrete numerical model for granular assemblies, Geotechnique **29**, 47 (1979).
[2] G. Kuwabara and K. Kono, Restitution coefficient in a collision between two spheres, Jpn. J. Appl. Phys. **26**, 1230 (1987).
[3] Y. Tsuji, T. Tanaka, and T. Ishida, Lagrangian numerical simulation of plug flow of cohesionless particles in a horizontal pipe, Powder Technol. **71**, 239 (1992).
[4] N. V. Brilliantov, F. Spahn, J. M. Hertzsch, and T. Poschel, Model for collisions in granular gases, Phys. Rev. E **53**, 5382 (1996).
[5] A. D. Renzo and F. P. D. Maio, Comparison of contact-force models for the simulation of collisions in DEM-based granular flow codes, Chem. Eng. Sci. **59**, 525 (2004).
[6] A. D. Renzo and F. P. D. Maio, An improved integral nonlinear model for the contact of particles in disctinct element simulations, Chem. Eng. Sci. **60**, 1303 (2005).
[7] A. B. Stevens and C. M. Hrenya, Comparison of soft-sphere models to measurements of collision properties during normal impacts, Powder Technol. **154**, 99 (2005).
[8] N. V. Brilliantov, N. Albers, F. Spahn, and T. Poschel, Collision dynamics of granular particles with adhesion, Phys. Rev. E **76**, 051302 (2007).
[9] C. Thornton, S. J. Cummins, and P. W. Cleary, An investigation of the comparative behavior of alternative contact force models during elastic collisions, Powder Technol. **210**, 189 (2011).
[10] C. Thornton, S. J. Cummins, and P. W. Cleary, An investigation of the comparative behavior of alternative contact force models during inelastic collision, Powder Technol. **233**, 30 (2013).
[11] Y. Q. Feng, B. H. Xu, S. J. Zhang, A. B. Yu, and P. Zulli, Discrete particle simulation of gas fluidization of particle mixtures, AIChE J. **50**, 1713 (2004).
[12] B. Remy, J. G. Khinast, and B. J. Glasser, Discrete element simulation of free flowing grains in a four-bladed mixer, AIChE J. **55**, 2035 (2009).
[13] E. W. C. Lim, C. H. Wang, and A. B. Yu, Discrete element simulation for pneumatic conveying of granular material, AIChE J. **52**, 496 (2006).
[14] M. Farrell, C. K. K. Lun, and S. B. Savage, A simple kinetic theory for granular flow of binary mixtures of smooth, inelastic, spherical particles, Acta Mech. **63**, 45 (1986).
[15] S. R. Dahl, R. Clelland, and C. M. Hrenya, The effects of continuous size distributions on the rapid flow of inelastic particles, Phys. Fluids **14**, 1972 (2002).
[16] M. W. Weber, D. K. Hoffman, and C. M. Hrenya, Discrete-particle simulations of cohesive granular flow using a square-well potential, Granul. Matter **6**, 239 (2004).
[17] C. K. K. Lun and S. B. Savage, A simple kinetic theory for granular flows of rough, inelastic spherical particles, ASME J. Appl. Mech. **54**, 47 (1987).
[18] V. Kumaran, Velocity distribution function for a dilute granular material in shear flow, J. Fluid Mech. **340**, 319 (1997).
[19] A. N. Volkov, Y. M. Tsirkunov, and B. Oesterle, Numerical simulation of a supersonic gas–solid flow over a blunt body: The role of interparticle collisions and two-way coupling effects, Int. J. Multiph. Flow **31**, 1244 (2005).
[20] J. M. Link, N. G. Deen, J. A. M. Kuipers, X. Fan, A. Ingram, D. J. Parker, J. Wood, and J. P. K. Seville, PEPT and discrete particle simulation study of spout-fluid bed regimes, AIChE J. **54**, 1189 (2008).
[21] A. Kosinska, B. V. Balakin, and P. Kosinski, Theoretical analysis of erosion in elbows due to flows with nano- and micro-size particles, Powder Technol. **364**, 484 (2020).
[22] E. T. Whittaker, *A Treatise on the Analytical Dynamics of Particles and Rigid Bodies* (Cambridge University Press, Cambridge, 1904).
[23] W. J. Stronge, *Impact Mechanics* (Cambridge University Press, Cambridge, 2000).
[24] W. J. Stronge, Smooth dynamics of oblique impact with friction, Int. J. Impact Eng. **51**, 36 (2013).
[25] S. Djerassi, Collision with friction; Part A: Newton's hypothesis, Multibody Syst. Dyn. **21**, 37 (2009).
[26] S. Djerassi, Collision with friction; Part B: Poisson's and Stornge's hypotheses, Multibody Syst. Dyn. **21**, 55 (2009).
[27] R. M. Brach, Friction, restitution, and energy loss in planar collisions, ASME J. Appl. Mech. **51**, 164 (1984).
[28] R. M. Brach, Rigid body collisions, ASME J. Appl. Mech. **56**, 133 (1989).
[29] J. B. Keller, Impact with friction, ASME J. Appl. Mech. **53**, 1 (1986).

[30] B. Oesterle and A. Petitjean, Simulation of particle-to-particle interactions in gas-solid flow, Int. J. Multiph. Flow **19**, 199 (1993).
[31] C. T. Crowe, *Multiphase Flow Handbook* (CRC Press, Boca Raton, FL, 2005).
[32] P. Kosinski and A. C. Hoffmann, An extension of the hard-sphere particle-particle collision model to study agglomeration, Chem. Eng. Sci. **65**, 3231 (2010).
[33] A. Kosinska, Interaction of debris with a solid obstacle: Numerical analysis, J. Hazard. Mater. **177**, 602 (2010).
[34] O. R. Walton, Numerical simulation of inelastic frictional particle-particle interactions, in *Particulate Two-Phase Flow*, edited by M. C. Rocco (Butterworth-Heinemann, Boston, 1993).
[35] S. F. Foerster, M. Y. Louge, H. Chang, and K. Allia, Measurements of the collision properties of small spheres, Phys. Fluids **6**, 1108 (1994).
[36] B. P. B. Hoomans, J. A. M. Kuipers, W. J. Briels, and W. P. M. van Swaaij, Discrete particle simulation of bubble and slug formation in a two-dimensional gas-fluidised bed: A hard-sphere approach, Chem. Eng. Sci. **51**, 99 (1996).
[37] N. G. Deen, M. van Sint Annaland, M. A. van der Hoef, and J. A. M. Kuipers, Review of discrete particle modeling of fluidized beds, Chem. Eng. Sci. **62**, 28 (2007).
[38] M. W. Weber and C. M. Hrenya, Square-well model for cohesion in fluidized beds, Chem. Eng. Sci. **61**, 4511 (2006).
[39] P. Kosinski and A. C. Hoffmann, Extension of the hard-sphere particle-wall collision model to account for particle deposition, Phys. Rev. E **79**, 061302 (2009).
[40] P. Kosinski and A. C. Hoffmann, Extended hard-sphere model and collisions of cohesive particles, Phys. Rev. E **84**, 031303 (2011).
[41] K. L. Johnson, *Contact Mechanics* (Cambridge University Press, Cambridge, 1985).
[42] O. R. Walton and R. L. Braun, Viscosity, granular-temperature, and stress calculations for shearing assemblies of inelastic, frictional disks, J. Rheol. **30**, 949 (1986).
[43] C. Thornton, Coefficient of restitution for collinear collisions of elastic-perfectly plastic spheres, ASME J. Appl. Mech. **64**, 383 (1997).
[44] E. Falcon, C. Laroche, S. Fauve, and C. Coste, Behavior of one inelastic ball bouncing repeatedly off the ground, Eur. Phys. J. B **3**, 45 (1998).
[45] R. Ramirez, T. Poschel, N. V. Brilliantov, and T. Schwager, Coefficient of restitution of colliding viscoelastic spheres, Phys. Rev. E **60**, 4465 (1999).
[46] F. P. D. Maio and A. D. Renzo, Analytical solution for the problem of frictional-elastic collisions of spherical particles using the linear model, Chem. Eng. Sci. **59**, 3461 (2004).
[47] N. Maw, J. R. Barber, and J. N. Fawcett, Oblique impact of elastic spheres, Wear **38**, 101 (1976).
[48] A. Kharaz, D. A. Gorham, and A. D. Salman, An experimental study of the elastic rebound of spheres, Powder Technol. **120**, 281 (2001).
[49] H. Kruggel-Emden, S. Wirtz, and V. Scherer, An analytical solution of different configurations of the linea viscoelastic and frictional-elastic tangential contact model, Chem. Eng. Sci. **62**, 6914 (2007).
[50] P. Kosinski, B. V. Balakin, P. Middha, and A. C. Hoffmann, Heat conduction during collisions of cohesive and viscoelastic particle, Int. J. Heat Mass Transf. **58**, 107 (2013).
[51] P. Kosinski, B. V. Balakin, P. Middha, and A. C. Hoffmann, Collisions between particles in multi- phase flows: Focus on contact mechanics and heat conduction, Int. J. Heat Mass Transf. **70**, 674 (2014).
[52] E. Buckingham, On physically similar systems; illustrations of the use of dimensional equations, Phys. Rev. **4**, 345 (1914).
[53] K. H. Hunt and F. R. E. Crossley, Coefficient of restitution interpreted as damping in vibroimpact, J. Appl. Mech. **42**, 440 (1975).
[54] J. Lee and H. J. Herrmann, Angle of repose and angle of marginal stability: molecular dynamics of granular particles, J. Phys. A **26**, 373 (1993).